

**IMECE2018-87324**

## DESIGN OF A DUCTED CROSS-FLOW TURBINE FOR MARINE CURRENT ENERGY EXTRACTION

**Jai N. Goundar**

The University of the South Pacific  
Suva, Fiji

**Deepak D. Prasad**

The University of the South Pacific  
Suva, Fiji

**Mohammed Rafiuddin Ahmed**

The University of the South  
Pacific  
Suva, Fiji

### ABSTRACT

Marine current energy is a clean energy source and is a solution to the problems faced by burning fossil fuels such as global warming and climate change. Once tapped, the useful shaft power can be converted into electrical energy. To make this practical, the designed energy converter should be capable of operating at low marine current velocities, it should be suitable for installation at locations that have low water depths and should have lower manufacturing, installation and maintenance costs. A ducted cross-flow turbine has all the above features and it will be suitable for Pacific Island countries (PICs) for extracting marine current energy. The ducted cross-flow turbine was designed, modelled and analyzed in commercial Computational Fluid dynamic (CFD) code ANSYS-CFX. The inlet and outlet duct sizes were optimized for maximum output. Before the analysis of full model, the CFD results were validated with experimental results. Simulations for the 1:10 ducted cross-flow turbine (having a diameter of 150 mm) were performed with 400,000 nodes, as increase in the grid size did not make much difference other than increasing the simulation time significantly. The maximum difference in the power coefficient between CFD and experimental results was 6%. Simulations were then performed for the full-scale prototype, which has a duct (nozzle) inlet of 3.5 m x 3.5 m and a turbine diameter of 1.5 m, at three freestream velocities of 0.65 m/s, 1.95 m/s and 3.25 m/s. Analysis of the prototype performance showed that the ducted cross-flow turbine can reach a maximum efficiency of 56% and can produce 21.5 kW of power at a current speed of 1.95 m/s and 103.6 kW at 3.25 m/s. The designed cut-off speed was 4 m/s.

### NOMENCLATURE

|                |   |   |
|----------------|---|---|
| A              | = | Cross sectional area of the turbine (m <sup>2</sup> ) |
| CFD            | = | Computational fluid dynamics                          |
| C <sub>P</sub> | = | Power coefficient = $P / (0.5\rho AU^3)$              |
| DCFT           | = | Ducted cross-flow turbine                             |
| FEA            | = | Fiji Electricity Authority                            |
| HAWT           | = | Horizontal axis wind turbine                          |
| HAMCT          | = | Horizontal axis marine current turbine                |
| P              | = | Rotor shaft power = $T \times \Omega$ (watts, W)      |
| PIC            | = | Pacific Island Countries                              |
| T              | = | Rotor torque (N.m)                                    |
| TSR            | = | Tip speed ratio                                       |
| U              | = | Freestream velocity (m/s)                             |
| $\Omega$       | = | Angular speed of rotor (rad/s)                        |
| $\alpha$       | = | Convergence/divergence angle (deg)                    |
| $\rho$         | = | Sea water density (1020 kg/m <sup>3</sup> )           |

### INTRODUCTION

Many countries around the world are trying to meet their energy needs with renewable energy resources. The challenge is how much we can extract and how long the energy harvesting device can last. The growing energy demand is making it difficult to meet all the energy needs by renewable energy resources. On the other hand, extracting fossil fuels is becoming expensive; most of the easily available fossil fuels have already been extracted. This has resulted in an increase in fuel prices. The fuel price further increases as it gets transported to the Pacific Island countries (PIC) like Fiji. Most of the imported fuels are used for transportation and to generate

electricity for the country. Fiji Electricity Authority (FEA) burned about 97,205 tons of diesel and heavy fuel oil in 2014 meeting 51% of electricity demand and the remaining 49% was met by renewable energy and independent power producers [1]. The increase in fuel price over the years and increasing electricity demand has encouraged Fiji to meet energy demand using renewable energy resources. Fiji is already focusing on producing electricity using hydro-power, wind power and solar power. Energy generated from different energy sources can be fed into the grid to keep the local electricity grid energized. Marine current energy is one of the most reliable forms of ocean energy and can be utilized efficiently to generate electricity. There are many marine current channels and stream around Fiji Islands. These can be utilized to meet the nation's energy requirements.

Lot of work has been done by many researchers in designing and developing marine current energy harvesting devices. Horizontal axis marine current turbines (HAMCT) are currently at the pre-commercial stage. The turbines can attain maximum efficiency up to 45–48% at the design operating conditions [2-7]. However, there are many challenges in terms of installing HAMCTs in Small Island countries like Fiji. Firstly, the manufacturing, installation and maintenance costs of HAMCT: Fiji does not have advanced manufacturing industries to manufacture the complex geometry of HAMCT blades and other components; hence it will be required to import the whole unit system. Also, the installation and maintenance of the turbine needs to be done by trained and qualified personnel; experts from other countries will be required to do those specific works. This will further increase the cost. Secondly, the complex operating system of HAMCT, the lift generated by the blade sections contributes towards the operation of the turbine. For the turbine to perform to its expectation, it will have to operate under ideal conditions; unfavorable conditions will affect the turbine's performance. The performance of HAMCT significantly deteriorates in highly turbulent flows and when blade fouling occurs [8]. Occurrence of cavitation is very common in lift-governed turbines. Lift is generated when local pressure on one side of the blade is significantly lower compared to the other side of the blade. If the local pressure on the blade drops below vapor pressure, it will cause the water to vaporize and the collapsing bubbles adversely affect the turbine's performance. The momentum of collapsing bubble is high enough to causes structural failures in metals over the period of time [9]. To overcome the above challenges and to design a suitable and feasible marine current turbine for Fiji, a totally new design approach was followed and a ducted cross-flow turbine was designed.

Cross-flow turbines are not very commonly used; their applications are restricted to specific operating conditions. However, a lot of research work has been done by researchers for design and development of cross-flow turbines for hydro power generation; some of these works are presented in references [10-12]. For hydropower generation using cross-

flow turbines, water is normally delivered from a height and the turbine efficiency can easily exceed 60% [13-14]. For an isolated turbine placed in an open channel, the maximum efficiency can be around 59%, according to the Betz criteria [15-16]. Numerical analysis performed on a cross-flow turbine designed by Kim et al. [17] for wave energy extraction had a maximum efficiency of 51%. Theoretical and experimental works carried out by researchers suggest that the efficiency of an isolated turbine in an open channel can be further improved by placing a duct or augmentation channel around the turbine. The placement of the duct reduces the pressure at the back of the turbine, hence drawing more fluid into the duct and increasing the efficiency. The increase in the turbine's performance should be significant to compensate for the added cost of the duct. Researchers have found that the efficiency of an isolated turbine can be improved by 70% [18, 19]. A performance study was conducted by Kirke et al. [20] on Darrieus hydrokinetic turbine with and without the diffuser. Without the diffuser, the power coefficient ( $C_p$ ) of the turbine was between 0.1 to 0.25; when a duct was placed around the turbine, the  $C_p$  of the turbine increased to 0.3 to 0.45.

The present paper presents the detailed design of a ducted cross-flow turbine (DCFT) tailor-made for Fiji. When designing the DCFT, the manufacturing, installation and maintenance costs were taken in to consideration and were kept as low as possible. The performance of the ducted cross-flow turbine was analyzed using ANSYS-CFX. Before modeling the full prototype, a scaled-down model of the turbine was fabricated and tested in a water channel to validate the numerical results. The numerical analysis of the prototype was then performed and the performance parameters of the turbine were computed. The results show that the turbine can reach a maximum numerical efficiency of around 56% and can produce power of 21.5 kW and 103.6 kW at freestream velocities of 1.95 m/s and 3.25 m/s respectively. The turbine starts producing power at a very low speed of around 0.65 m/s.

## METHODOLOGY

To design an efficient and suitable turbine for any location, marine current resource assessment is necessary to determine turbine geometry and its operating parameters. Therefore, marine current resource assessment was performed for this location. The assessment site was at coral coast, Sigatoka, and is called the Gun-barrel passage. The marine current was measured using Argonaut aqua-dopp current profiler (accuracy:  $\pm 0.01$  m/s). The assessment results show that the site has a combination of both tidal current and rip current. The marine current speed easily exceeded 2.5 m/s during high wave activity. The measurements were performed for 3 lunar months and the average current speed was around 0.85 m/s for the recorded time period [7]. The depth of the passage increases from 10 m to 25 m as we move seawards; likewise, the width also varies from 5 m to 15 m, the depth of the passage was measured using depth profiler installed with fish finder

(accuracy:  $\pm 0.1$  m). During the rip current, the flow becomes very turbulent.

It is important to design an efficient marine current turbine that performs well and survives the harsh sea conditions. One of the most appropriate marine current energy converters for this case and for other locations that have marine current streams like the above can be a DCFT. A conceptual design and the features of a ducted cross-flow turbine are shown in Fig. 1. It has two main components – a cross-flow turbine and a duct. The cross-flow turbine converts kinetic energy from marine currents into shaft power. The cross-flow turbine is similar in appearance to the one used for hydro power energy conversion. However, the guide vanes, blade geometry and blade angles are normally optimized for marine current flow conditions. The duct reduces the pressure at the turbine exit, hence increasing the flow through the turbine. The DCFT has 3 main components: the nozzle (with the guides) that accelerates the flow and guides the flow smoothly on to the turbine blades; the second important component is the turbine, and the third important component is the diffuser with its guides; the diffuser further reduces the pressure at the turbine exit, which increases the turbine output.

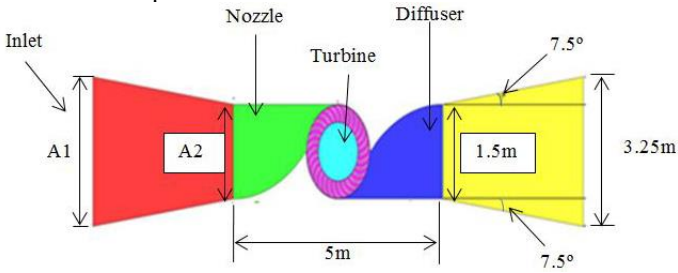


Fig. 1 Schematic of ducted cross-flow turbine.

The ducted cross-flow turbine has simple geometrical components; therefore manufacturing of DCFT in Fiji is feasible. Fiji and other pacific island countries do not have advanced manufacturing systems and experts to do the installation of complicated marine current turbines like HAMCT, as mentioned earlier. If the DCFT is installed at low water depths, then the generator mountings can be elevated above the water level for regular maintenance work.

The turbine size and its operating parameters were determined from assessment results. Other turbine geometric parameters were optimized to maximize the power and to reduce the material cost. The duct inlet area  $A_1$  is  $11.22 \text{ m}^2$  ( $3.5 \text{ m} \times 3.5 \text{ m}$ ); this inlet area takes up 25% of the marine current stream area. The inlet-to-throat area and exit-to throat-area ratio ( $A_1/A_2$ ) was optimized to have good balance between the power output, material and reinforcement costs during manufacturing. Performance analysis was done for area ratios ( $A_1/A_2$ ) of 2, 3, 4, 5, 6 and 7; from the results, the optimum output was between the area ratios of 5-6. Further analysis was carried out for area ratios ranging from 5 to 6 at the intervals of 0.1 and the optimum area ratio came to 5.4. To further optimize

the duct, the convergence angle (inlet to throat) and divergence angle (throat to exit) were also optimized. Simulations were run at different angles ranging from  $7^\circ$  to  $24^\circ$  and optimum angle came to  $15^\circ$ . The guides were designed in a way so that the water enters the turbine blades without shock and without creating any swirling motion and eddies. Other details and dimensions of the turbine are shown in Fig. 2. The cross-flow turbine consists of 30 blades with entry angle of  $30^\circ$ . The turbine diameter and height are both 1500 mm. The 2 guides at the inlet and exit have a curvature radius of 2372 mm and a length of 1740 mm.

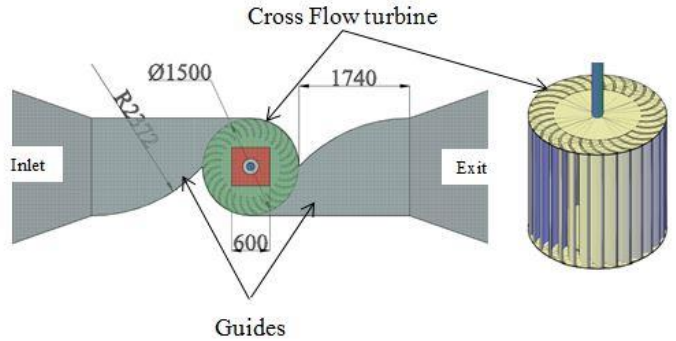


Fig. 2 Dimensions of the duct and the turbine in mm.

A model of the DCFT of scale 1:10 was constructed. The scale was chosen based on the channel dimensions and the flow conditions in which the DCFT was to be tested. Froude scaling was used to obtain the geometrical dimensions of the model. The channel has a natural water stream of  $0.8 \times 0.8 \text{ m}$  cross-section and was approximately 5 m in length. It is located at the coast of Laucala bay Suva, Fiji. The average flow velocity at the time of measurements was 1.04 m/s. The stream at the test site represented near-same flow conditions as for the actual device. The duct was fabricated using 3 mm clear Perspex riveted together and sealed with clear silicone gel. The blades were fabricated with 3 mm aluminum sheets. Figure 3 shows the 1:10 model of the cross-flow turbine for experimental testing.

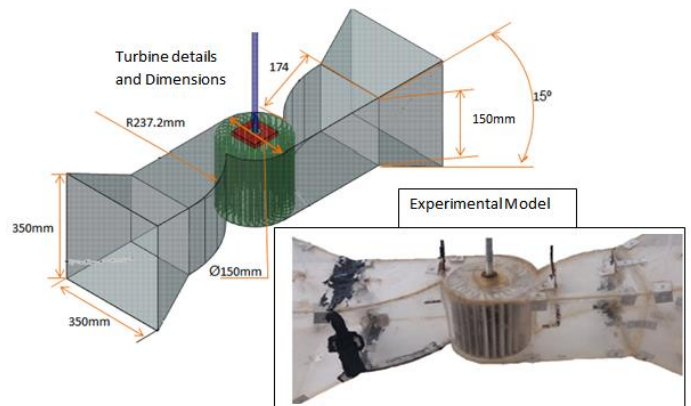


Fig. 3 Photograph and schematic of the 1: 10 experimental model with dimensions.

A torque sensor and an rpm sensor were used for measuring the torque ( accuracy:  $\pm 0.01$  kgf.cm) and rotational speed (accuracy:  $\pm 0.01$ rpm). The turbine was allowed to spin and torque was measured for 5 different turbine speeds (revolutions per minutes (rpm)). From the results, the power coefficient was calculated and the results were compared with numerical results.

The 3-D ducted cross-flow turbine was modeled using UniGraphics NX 4 package and then imported in to Ansys ICEM CFD for meshing. Hexahedral grids were used for meshing purposes. This technique allows for user-defined meshing and ensures that the grid is appropriate to capture the important flow phenomena accurately. The initial model was of the same size as the experimental model. Once the meshing was done, then the model was imported into CFX Pre to define boundary conditions, interfaces and other initial parameters for the simulation. The main domain was sub-divided into subdomains as shown in Fig. 4. The specified sub-domains are *INLET*, *OUTLET*, *NOZZLE*, *DIFFUSER* and *TURBINE*. The nozzle and diffuser were specified as stationary solid walls with no-slip boundary condition.

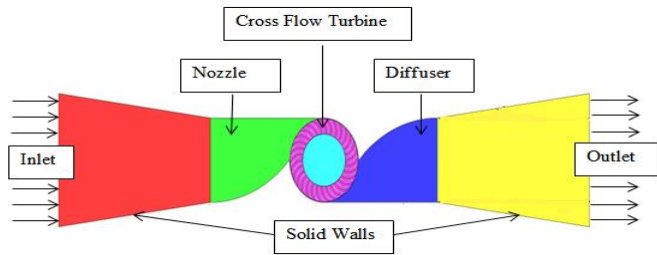


Fig. 4 Domains created for specifying the boundary conditions.

The inlet was assigned an inlet velocity for each simulation based on the TSR. The exit was assigned a relative pressure to 0 Pa. The turbine was allowed to rotate about its rotational axis with specified rotational velocity. Finally appropriate interface regions were created; for the interfaces automatic mesh connections were used. The simulations were run on a computer which had Intel Core i7 processor and 8 GB RAM. An additional graphics card of 8 GB was also installed. The basic equations for viscous flow that are solved by ANSYS – CFX are the mass and momentum conservation equations:

$$\frac{\partial \rho}{\partial t} + \nabla \cdot (\rho U) = 0 \quad (1)$$

$$\frac{\partial}{\partial t} \rho v + \nabla \cdot \rho v = -\nabla p + \nabla \cdot \tau = 0 \quad (2)$$

where  $\tau$  is the stress tensor and related to the strain rate by:

$$\tau = \mu \left( \nabla U + (\nabla U)^T - \frac{2}{3} \delta \nabla \cdot U \right) \quad (3)$$

The simulation type was transient to capture the rotor-fluid interaction more accurately. Shear stress transport (SST) turbulence model was employed for the simulations. Time discretization of the equations was accomplished using the second order backward Euler scheme. The inlet velocity was assigned at 0.832 m/s. The inlet velocity drops by 20% compared to the freestream velocity. This was determined during model testing. For the ANSYS-CFX solver, high resolution advection scheme was selected. Maximum coefficient loop was set to 10 for convergence control. The torque was calculated for each time step for the given rpm, and simulations continued until the torque value converged. To check on the accuracy, the results obtained numerically were compared with the experimental data and the comparison of results is shown in the next section.

## RESULTS AND DISCUSSION

### *Part A – Validation*

Firstly, it was important to study the influence of grid size on numerical results. In order to conduct grid independence test, three different grids with approximately 250,000, 400,000 and 500,000 nodes were employed. For all the simulations, the turbine power was monitored. The turbine powers obtained for 250,000, 400,000 and 500,000 nodes were 21230 W, 21095 W and 21089 W respectively. A grid size of 400,000 nodes was selected for the simulation as further increase in the grid size did not make much difference apart from increasing the simulation time. Figure 5 shows the results obtained by experimentation and CFD for the 1:10 DCFT model. The experiments were performed at five different TSR; the simulations were also carried out at the same five TSR.

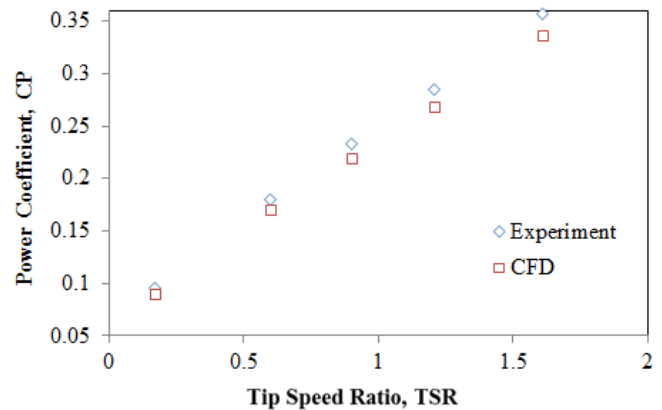


Fig. 5 Power coefficient obtained from experiments and CFD.

The results show that at low TSR, the experimental and computational results matched reasonably well. The highest Cp value obtained from CFD is about 6% lower compared to the experimental value. The difference is mainly due to mechanical losses for the experimental case. These losses are mostly due to



friction, vortices and unsteady flows cause by sharp edges left during fabrication of experimental model. Considering the overall good agreement between the two, it was concluded that CFD can be effectively used for predicting the performance of the ducted cross-flow turbines if same conditions are used.

Part B – Performance of Full Scale Model

For the performance analysis of the full scale DCFT, the numerical method was same as in the validation case. The only difference was in the inlet velocities. The inlet velocities were 0.52 m/s, 1.56 m/s and 2.6 m/s which correspond to freestream velocities of 0.65 m/s, 1.95 m/s and 3.25 m/s respectively. These velocities were selected based on assessment results. The velocity vectors in the DCFT at the inlet velocity of 1.56 m/s are shown in Fig. 6.

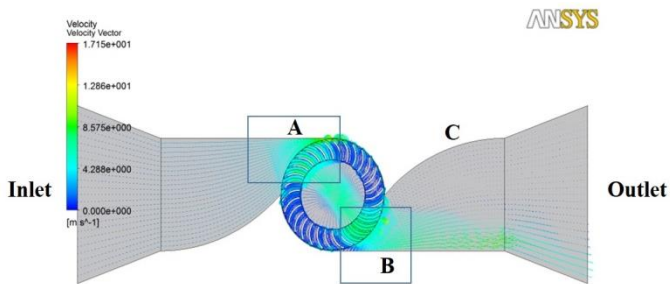


Fig. 6 Velocity vectors in the turbine.

The flow accelerates from the inlet and a high energy flow is observed at the nozzle exit near region A. As the flow passes through the set of blades in region A, it imparts energy to the turbine. Since the area reduces between the blade passages, the flow further accelerates before imparting energy onto the blades in region B, as can be seen from Fig. 7. It can also be seen that when the fluid strikes the blades in the region B, it exerts a force on the blades and hence, impulse action also plays a role in the energy transfer. This flow is termed as cross-flow and is responsible for improved turbine performance.

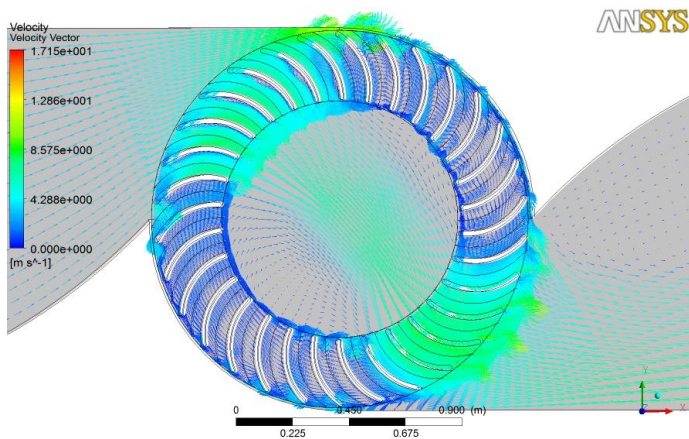


Fig. 7 The changes in the water velocity as it flows over the blades.

In region C, recirculating flow is observed. The size of the vortex typically has a direct influence on the turbine’s performance. Also, in the figure, increase in the local velocity after the flow exits the turbine blades has been captured. Similar performance and flow characteristics were reported in the works of Prasad et al. [21] and Kim et al. [17].

The pressure variation was also obtained using CFX. Figure 8 shows the pressures at different sections of the DCFT. It can clearly be seen that the pressure downstream of the turbine is less than the upstream pressure. This makes more flow to enter the duct and the turbine and increases the power output and efficiency.

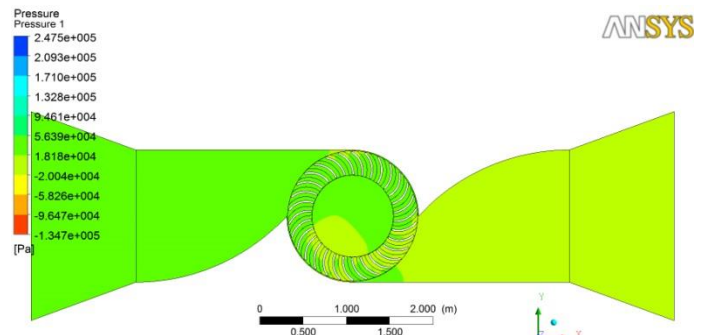


Fig. 8 Pressures at different sections of the DCFT.

The power coefficient was calculated from the power output computed from numerical analysis. The torque was measured for freestream velocities of 0.65 m/s, 1.95 m/s and 3.25 m/s. For each of the velocities, simulations were performed for TSR from 1–3.5 at intervals of 0.25. The coefficient of power at different freestream velocities and at different TSR is shown in Fig. 9. The turbine can reach the maximum efficiency of 54% at TSR of 3.2 for the freestream velocity of 0.65 m/s producing 0.8 kW and for 1.95 m/s producing around 21.5 kW. The efficiency slightly increases to 56% for the freestream velocity of 3.25 m/s producing around 103.6 kW of shaft power. The power produced by the turbine increases with increasing TSR, reaches a maximum and then drops significantly. The peak indicates that the energy imparted by the fluid is maximum and hence the turbine produces peak power. The drop in the turbine performance from this point onwards indicates the interaction between the incoming flow and the turbine is no longer optimal and leads to drop in power production.

The cut-in speed of the turbine was intended to be as low as possible so that the turbine starts producing power at low marine current velocity. From the assessment results, the marine current velocity was around 0.5 m/s for a considerable part of the day; therefore the design ensured that the turbine starts producing power at 0.5 m/s. The cut-off velocity for the designed turbine is 4 m/s to prevent the turbine from structural damage.

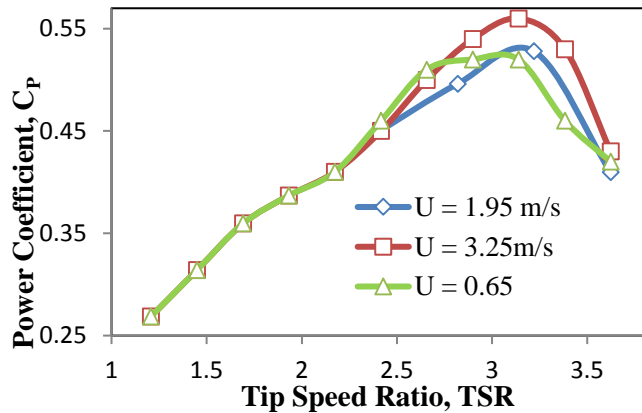


Fig. 9 The power coefficient of the turbine at freestream velocities from 0.65 m/s to 3.25 m/s.

## CONCLUSIONS

The concept of tapping marine current energy using ducted cross-flow turbines is relatively new. The design and performance analysis of a ducted cross-flow turbine was successfully carried out. This turbine has many advantages such as low cost of production and maintenance. This turbine will be very suitable for Fiji and other PICs for electricity generation. It also has other advantages such as: the chances of cavitation are reduced for this type of turbine and it can be installed in channels with lower depth which is not possible with lift-governed turbines. The duct inlet area  $A_1$  takes up 25% of the marine current stream area. The inlet-to-throat area and exit-to-throat-area ratio ( $A_1/A_2$ ) was optimized to have good balance between the power output, material and reinforcement costs during manufacturing. An optimum area ratio of 5.4 was obtained. The convergence and divergence angles were also optimized. A 1:10 scaled model of the DCFT was fabricated and tested for validating the CFD results. After the validation, simulations were performed on the full-scale prototype, which has a duct (nozzle) inlet of 3.5 m x 3.5 m and a turbine diameter of 1.5 m, at three freestream velocities of 0.65 m/s, 1.95 m/s and 3.25 m/s. The designed turbine has a peak efficiency ranging from 54% to 56% and produces power of 21.5 kW and 103.6 kW at freestream velocities of 1.95 m/s and 3.25 m/s respectively. This is a reasonable power output for such system to be feasible and to be commercially viable.

## REFERENCES

[1] "Fiji Electricity authority; annual report 2014, 2016", available online at [www.fea.com.fj/pages.cfm/downloads/annualreports.html](http://www.fea.com.fj/pages.cfm/downloads/annualreports.html), accessed 3<sup>rd</sup> October 2017.

[2] Batten, W.M.J., Bahaj, A.S., Molland, A.F. and Chaplin, J.R., 2006, The Prediction of Hydrodynamic Performance of Marine Current Turbines, *Renewable Energy*, 33, pp. 1085-1096.

[3] Sale, D., Jonkman, J. and Musial, W., 2009, Hydrodynamic Optimization Method and Design Code for Stall-Regulated Hydrokinetic Turbine Rotor, National Renewable energy laboratory.

[4] Nicholls-Lee, R.F., Turnock, S.R. and Boyd, S.W., 2008, Simulation Based Optimisation of Marine Current Turbine Blades, *Proceedings of the 7th International Conference on Computer and IT Applications in the Maritime Industries*, Belgium.

[5] Goundar, J.N., Ahmed, M.R. and Lee, Y.H., 2012, Numerical and Experimental Studies on Hydrofoils for Marine Current Turbines, *Renewable Energy*, 42, pp. 173-179.

[6] Goundar, J.N. and Ahmed, M.R., 2013, Design of a Horizontal Axis Tidal Current Turbine, *Applied Energy*, 111, pp. 161-174.

[7] Goundar, J.N., and Ahmed, M.R., 2014, Marine Current Energy Resource Assessment and Design of a Marine Current Turbine for Fiji, *Renewable Energy*, 65, pp. 14-22.

[8] Maganga, F. and Germain, G., 2010, Experimental Characterisation of Flow Effects on Marine Current Turbine Behaviour and on its Wake Properties, *IET Renewable Power Generation*, 4, pp. 498-509.

[9] Jones, J.A., and Chao, Y., 2009, Offshore Hydrokinetic Energy Conversion for Onshore Power Generation. *Proceedings of the ASME 28th International Conference On Ocean, Offshore and Arctic Engineering (OMAE2009)*, Honolulu, Hawaii, May 31–June 5.

[10] Khosrowpanah, S, Fiuzat, A.A. and Albertson, M.L., 1988, Experimental Study of Cross-Flow Turbine, *Journal of Hydraulic Engineering*, 114, pp. 299-314.

[11] Fiuzat A.A. and Akerkar, B.P., 1991, Power Outputs of Two stages of Cross-Flow Turbine Efficiency, *Journal of Energy Engineering*, 117, pp. 57-70.

[12] Desai, V.R. and Aziz, N.M., 1994, An Experimental Investigation of Crossflow Turbine Efficiency, *Journal of Fluids Engineering*, 116, pp. 545-550.

[13] Choi, Y.D., Lim, J.I., Kim, Y.T. and Lee, Y.H., 2008, Performance and internal Flow Characteristics of a cross-Flow Hydro Turbine by the Shapes of Nozzle and Runner Blade, *Journal of Fluid Science and Technology*, 3, pp. 398-409.

[14] Olgun, H., 1998, Investigation of the Performance of a Cross-flow Turbine, *International Journal of Energy Research*, 22, pp. 953-964.

[15] Bergy, K.H., 1979, The Lanchester-Betz limit, *Journal of Energy*, 3, pp. 382-384.

[16] Gijs, A.M., 2007, The Lanchester-Betz-Joukowsky Limit. *Wind Energy*, 10, pp. 289-291.

[17] Kim, K.P., Ahmed, M.R. and Lee, Y.H., 2012, Efficiency Improvement of a Tidal Current Turbine Utilizing a Larger Area of Channel, *Renewable Energy*, 48, pp. 557- 564.

[18] Coiro, D.P., 2012, Development of Innovative Tidal Current Energy Converters: From Research to Deployment, *Asia-Pacific Forum on Renewable Energy (AFORE2012)*, South Korea.

[19] Khunthongjan, P. and Janyalertadun, A. 2012, A Study of Diffuser Angle Effect on Ducted Water Current Turbine Performance Using CFD, *Songklanakarin Journal of Science and Technology*, 34, pp. 61-67.

[20] Kirke, B.K., 2011, Tests on Ducted and Bare Helical and Straight Bladed Darrieus Hydrokinetic Turbines, *Renewable Energy*, 36, pp. 3013-3022.

[21] Prasad, D.D., Ahmed, M.R., and Lee, Y.H., 2014, Flow and Performance Characteristics of a Direct Drive Turbine for Wave Power Generation, *Ocean Engineering*, 81, pp. 39-49.